

Research highlights

Cite this: *Lab Chip*, 2013, 13, 1662
DOI: 10.1039/c3lc90025h

Šeila Selimović,^{ab} Mehmet R. Dokmeci^{ab} and Ali Khademhosseini^{*abcd}

www.rsc.org/loc

Happy-hour microfluidics

Microfluidic analysis methods utilizing optical or antibody-based detection are usually designed for biological samples such as protein solutions, cells, or body liquids. In this context, enzyme-linked immunosorbent assays (ELISA) have become a particularly useful analysis tool that is easily miniaturized and integrated into standard microfluidic devices.¹ However, microfluidic ELISA is rarely applied to sensing of toxic chemicals, particularly in agricultural, food and beverage industries. These fields could potentially benefit from utilizing microfluidics for screening and quality control tests, as recently demonstrated by Conde and co-workers.²

Novo *et al.*² developed a simple, U-shaped microfluidic channel structure and coupled it with chemiluminescent ELISA to detect and quantify the toxin ochratoxin A (OTA) in beer and wine. OTA is a natural product of fungi present in certain cereals (*e.g.* barley or hops) and grapes, and is therefore easily introduced into commercial products including alcoholic beverages. The wine and beer extracts (15 μ l each) tested by the authors were mixed with bovine serum albumin (BSA) and injected into the poly(dimethylsiloxane) (PDMS) chip with a syringe (Sample 1), along with a reference solution (Sample 2, Fig. 1). The mixture of BSA and OTA, if present in the samples, adsorbed onto PDMS, and was followed by a solution containing competitive primary and secondary antibodies tagged with horseradish peroxidase (HRP). In a period of 3 h these antibodies immobilized any unbound OTA, but also competed with BSA for OTA to capture even more toxin molecules. Finally, the commonly used chemical luminol was introduced into the chip to bind to the oxidizing agent HRP, thereby generating a blue chemiluminescent glow. To detect and analyze this optical signal, the microfluidic device had to be coupled with a chemiluminescence detector. In particular,

the PDMS device was placed on a glass platform, which contained a series of photodiodes characterized at 430 nm, the peak of the chemiluminescence signal. Thus, the more OTA that was present in the beer or wine sample, the more OTA was immobilized and enabled a chemiluminescent reaction, and the stronger the signal measured by the photodiodes. Quantitative values of the detected OTA concentrations were obtained by comparing the sample OTA contaminated results to the reference solution. The entire procedure was conducted at room temperature, which simplified the experimental protocol.

Of the tested beer and wine samples, some were deliberately spiked with OTA for calibration purposes. All beverages underwent an extraction process to remove antioxidants, which could bind non-specifically to OTA and to the antibodies and so generate false positive results. The tolerable daily intake (TDI) of OTA is considered to be on the order of ng

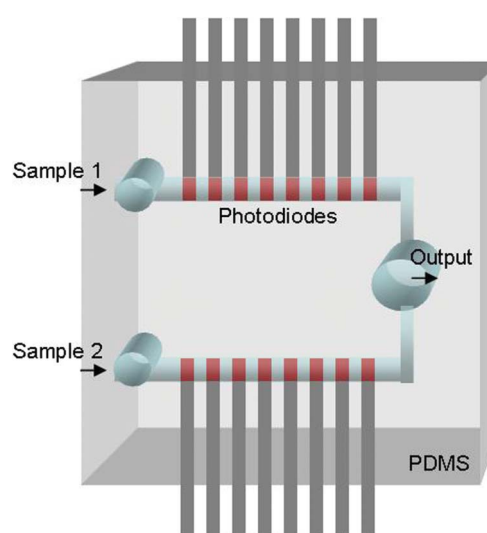


Fig. 1 Schematic of the microfluidic device for chemiluminescent ELISA. Sample 1 (OTA contaminated solution) and sample 2 (reference solution) are simultaneously introduced into the U-shaped microfluidic channel. Here, the OTA toxin contained in the samples is bound to preloaded antibodies, followed by luminol. The resulting chemiluminescent signal is captured by the photodiodes located below the microfluidic channel. Figure inspired by Novo *et al.*²

^aCenter for Biomedical Engineering, Department of Medicine, Brigham and Women's Hospital, Harvard Medical School, Cambridge, Massachusetts 02139, USA.

E-mail: alik@rics.bwh.harvard.edu

^bHarvard-MIT Division of Health Sciences and Technology, Massachusetts Institute of Technology, Cambridge, Massachusetts 02139, USA

^cWyss Institute for Biologically Inspired Engineering, Harvard University, Boston, Massachusetts 02115, USA

^dWorld Premier International – Advanced Institute for Materials Research (WPI-AIMR), Tohoku University, Sendai 980-8577, Japan

kg^{-1} of body weight, which determined the required sensitivity of the microfluidic ELISA.³ Indeed, the device was capable of detecting OTA concentrations on the order of 100 pg ml^{-1} in both beer and wine. This quantity is medically relevant, as it corresponds to the above listed TDI for an average-weight person drinking 2 glasses of wine or one glass of beer per day.

This work demonstrates the utility of microfluidics integrated with an optical detection platform as a technology suitable for inspecting food and beverage samples, and makes it an attractive system for research in agricultural and food industries. Furthermore, the device structure is sufficiently simple to allow for automated, large-scale production, and the chip is easy to use even by individuals without specialized training. Most importantly, the chip is compatible with a range of ELISA tests, such that even small breweries and wineries could use it to test their products for toxins before sale, carry out rapid inspection and avoid potential food poisoning accidents.

Chemical gradients using oscillating bubbles

Concentration gradients of chemicals, toxins, and even particles are a staple of microscale experiments that focus on screening a parameter space or optimizing experimental conditions. This is best seen in applications such as microfluidic protein crystallization or stem cell differentiation.^{4,5} In most cases the spatial concentration gradients are temporally static, and the stability of the gradients in time is seen as an advantage. However, some studies may require pulsatile gradients, where the amount of a chemical cue delivered to a sample changes with time, as is the case with cyclic toxin assays.⁶

To develop a well-controlled microfluidic system capable of generating and maintaining both temporally static and dynamic concentration gradients, Huang and colleagues have recently turned to acoustic waves as the control mechanism. Here, Ahmed *et al.*⁷ coupled a simple PDMS channel with an adjacent piezoelectric transducer capable of generating acoustic vibrations on the order of 10 kHz. The channel had two separate inputs, one for the sample (stimulant) and the other for the dilution medium (buffer). The two liquids mixed inside the channel, exiting through a common outlet. In the center of the channel 5 horseshoe-shaped structures were staggered, each of which trapped a bubble. The bubbles responded to the acoustic force from the transducer, and at an applied frequency of 30 kHz, they started to oscillate in unison. This resonance response led to the rapid movement of the two liquids near the bubbles (microstreaming), and then to their mixing (Fig. 2a). A single oscillation of a trapped bubble was recorded using a high-speed camera and is shown in Fig. 2b.

One particular observation led to the dynamic gradient generation. Namely, the oscillation amplitude of the trapped bubbles can be controlled in a linear manner by the voltage applied to the piezoelectric transducer. Furthermore, the mixing distance is found to depend linearly on the oscillation

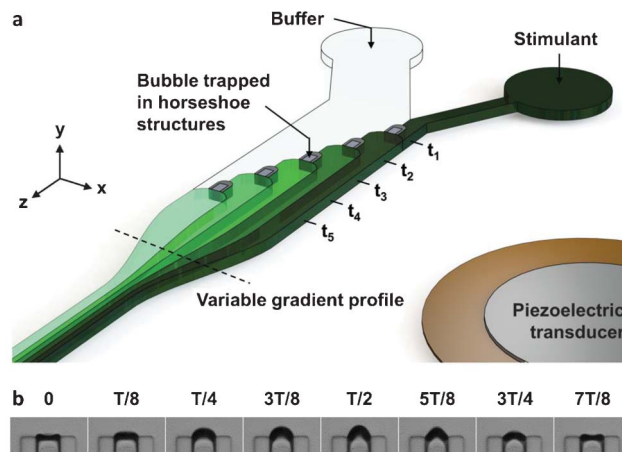


Fig. 2 Schematic of the microfluidic device for chemiluminescent ELISA. Figure reprinted with permission from the Royal Society of Chemistry from Ahmed *et al.*⁷

amplitude. Hence, by controlling the voltage that feeds into the transducer, it was possible to tune the mixing distance and the spatial shape of the concentration gradient. For example, an increase in applied voltage from 14 V to 17 V resulted in almost doubling the mixing distance to $\sim 250 \mu\text{m}$. Furthermore, making the applied potential time-dependent enabled the formation of temporally dynamic concentration gradients. For example, a sinusoidally time-dependent potential was able to produce cyclic changes in the concentration gradient. Importantly, the response of the gradient generator to changes in the potential was almost instantaneous, *de facto* enabling on-off switching of the concentration gradients.

The efficacy of the gradient generator was demonstrated using a mixture of PBS and FITC-dextran. Changing the applied voltage from 12 V to 16 V resulted in the generation of several concentration gradient profiles, some of which were shallow and resembled (at higher potentials) linear gradients, while others were sigmoidal. Yet others (at lower voltages) were similar to the diffusion-only mixing profiles. Thus, higher applied voltages resulted in a longer mixing distance and, hence, faster mixing. Cyclic (on-off) gradients could be successfully generated at frequencies of up to 0.1 Hz (not to be confused with the excitation frequency, which was on the order of kHz).

The proposed method of generating spatially and temporally dynamic concentration gradients can be easily integrated into a host of existing microfluidic devices, including cell-culture chips such as microwell arrays. For example, microwells loaded with analytes (protein droplets or cells) could be positioned inside the mixing channel, yet a distance away from the oscillating bubbles to avoid high, potentially damaging shear stresses. A major benefit of this device is its structural simplicity, as it does not rely on microvalves and micropumps as active mixers. Additionally, the footprint of this device is sufficiently small so that it can be combined with other devices without sacrificing much space. In the future, the observed

Highlight

microstreaming phenomenon could be applied to rapid mixing of liquids with vastly different viscosities, which otherwise relies on slow diffusive mixing.

Gold nanoparticle electrodes on paper for diagnostics

For the last two decades PDMS has been the material of choice for microfluidic devices, but in recent years paper has emerged for fabricating low-cost, portable diagnostic chips.⁸ Benefits of using paper for molecular analysis tests include that it can be locally treated with analytes, its wicking properties serve to transport liquid samples on-chip, and it can be patterned with wax to define and separate hydrophilic from hydrophobic regions. Furthermore, creative folding of paper can establish additional fluidic pathways, which is not possible with thicker PDMS devices. However, most paper devices have relied on biological receptors, such as enzymes or DNA, for molecular analysis. This approach is incompatible with long device shelf-lives, as the biological material can denature if not stored properly.

To address this shortcoming, the team of Yan and colleagues has explored the possibility of molecular imprinting of polymers on a paper substrate and coupling them with on-chip electrodes for analysis purposes. In its core, molecular imprinting serves to generate synthetic receptors for the analytes. This is accomplished by using the desired (biological) receptor as a template, around which a chemically interacting polymeric layer is formed. Then, the receptor is removed, leaving behind a cavity with the complementary shape, size, and molecular activity. Next, the analyte contained in a liquid sample can be bound onto the edge of this cavity. Molecular imprinting thus offers improved stability and specificity.

Ge *et al.*⁹ defined hydrophilic sample tab and paper auxiliary zones on the paper device (Fig. 3A) through wax patterning, then delivered carbon ink to portions of these hydrophilic patches to form working, counter, and reference electrodes (Fig. 3B and C). The sensitivity of the electrodes was increased by filling the attached porous paper with gold nanoparticles and growing a smooth (yet porous) gold layer on the paper sample zone within 10 min. Folding between the hydrophilic patches resulted in a 3D reservoir (6 mm diameter \times 0.18 mm height) that would become the detection region (electrochemical cell), by attaching a layer of molecularly imprinted polymer.

A type of glutamic acid (a neurotransmitter) was used as the biological template molecule and as the analyte. Different concentrations of the acid (on the order of 10–100 nM) in the form of spiked serum samples were dispensed onto the paper sample zone at room temperature. Then, the difference in current in response to a changing applied potential was recorded (differential pulse voltammetry, DPV). A steady-state was reached within \sim 4 min, indicating that the sample was fully absorbed within that time. This was an improvement

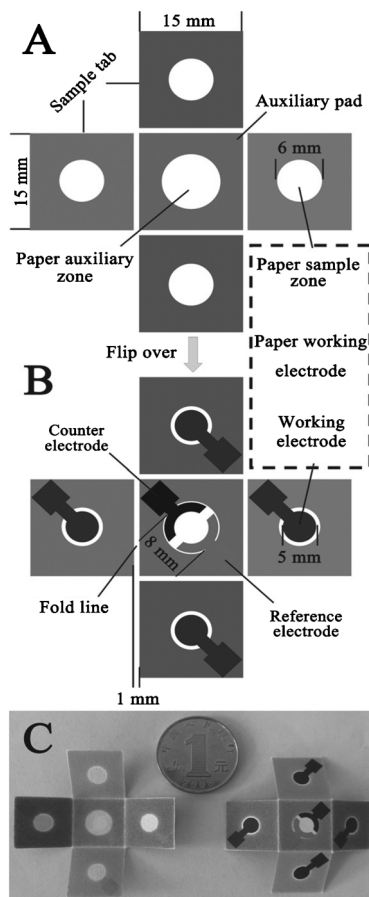


Fig. 3 Schematic of the paper microfluidic device containing porous Au-electrodes. The top side is shown in (A), the back side in (B). A photograph indicating the size of the open (unfolded) paper device is in (C). Figure reprinted with permission from Ge *et al.*⁹

compared to 10 min long absorption times on planar paper samples. The detection limit was found to be 2 nM of glutamic acid. Importantly, the same type of test was conducted on paper microdevices that had not been coated with gold nanoparticles. The sensitivity of this simpler device was one order of magnitude below that of the gold-containing chip. The importance of the molecularly imprinted polymer was also evaluated: in a control experiment the polymer was added to the chip, but without the biomolecular imprint, so that no binding sites for glutamic acid were present. In this case, no change in the recorded current was observed as a function of glutamic acid concentration.

The described study introduced molecular imprinting of polymers to paper microfluidic diagnostic devices. The sensitivity, specificity, and reproducibility data gained from this study indicates that molecular imprinting has the potential to revolutionize molecular analysis on paper. This is especially true, since molecular imprinting (instead of using biomolecules as receptors) also vastly increases the robustness and accuracy of the paper chips. Therefore, the proposed method may gain traction in the development of point-of-care

diagnostic devices and may be coupled with optical detection methods, such as chemiluminescence or colorimetry.

References

- 1 C.-C. Lin, J.-H. Wan, H.-W. Wu and G.-B. Lee, *J. Lab Autom.*, 2010, **15**, 253–274.
- 2 P. Novo, G. Moulas, D. M. França Prazeres, V. Chu and J. P. Conde, *Sens. Actuators, B*, 2013, **176**, 232–240.
- 3 *Scientific Panel on Contaminants in the Food Chain*, EFSA J, 2006, vol. 365, pp. 1–45.
- 4 Š. Selimović, F. Gobeaux and S. Fraden, *Lab Chip*, 2010, **10**, 1696–1699.
- 5 B. G. Chung, L. A. Flanagan, S. W. Rhee, P. H. Schwartz, A. P. Lee, E. S. Monuki and N. L. Jeon, *Lab Chip*, 2005, **5**, 401–406.
- 6 J. Atencia, G. A. Cooksey and L. E. Locascio, *Lab Chip*, 2012, **12**, 309–316.
- 7 D. Ahmed, C. Y. Chan, S.-C. S. Lin, H. S. Muddana, N. Nama, S. J. Benkovic and T. J. Huang, *Lab Chip*, 2013, **13**, 328–331.
- 8 X. Li, D. R. Ballerini and W. Shen, *Biomicrofluidics*, 2012, **6**, 011301.
- 9 L. Ge, S. Wang, J. Yu, N. Li, S. Ge and M. Yan, *Adv. Funct. Mater.*, 2013, DOI: 10.1002/adfm.201202785.